PL-TR-
97-1053

SPACECRAFT IDENTIFICATION BY MULTISPECTRAL SIGNATURE ANALYSIS USING NEURAL NETWORKS

Capt. Conrad J. Poelman
Stephanie R. Meltzer

March 1997

Final Report

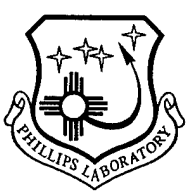

PHILLIPS LABORATORY
Advanced Weapons and Survivability Directorate
AIR FORCE MATERIEL COMMAND
KIRTLAND AIR FORCE BASE, NM 87117-5776

PL-TR-97-1053

Using Government drawings, specifications, or other data included in this document for any purpose other than Government procurement does not in any way obligate the U.S. Government. The fact that the Government formulated or supplied the drawings, specifications, or other data, does not license the holder or any other person or corporation; or convey any rights or permission to manufacture, use, or sell any patented invention that may relate to them.

This report has been reviewed by the Public Affairs Office and is releasable to the National Technical Information Service (NTIS). At NTIS, it will be available to the general public, including foreign nationals.

If you change your address, wish to be removed from this mailing list, or your organization no longer employs the addressee, please notify PL/WSA, 3550 Aberdeen Ave. SE, Kirtland AFB, NM 87117-5776.

Do not return copies of this report unless contractual obligations or notice on a specific document requires its return.

This report has been approved for publication.

Conrad J. Poelman

CONRAD J. POELMAN, Capt, USAF
Project Manager

FOR THE COMMANDER

Catherine J. Zeringue

CATHERINE J. ZERINGUE, Lt Col, USAF
Chief, Satellite Assessment Division

William G. Heckathorn

WILLIAM G. HECKATHORN, Col, USAF
Director, Advanced Weapons
and Survivability Directorate

REPORT DOCUMENTATION PAGE

Form Approved
OMB No. 0704-0188

1. AGENCY USE ONLY *(Leave blank)*	2. REPORT DATE	3. REPORT TYPE AND DATES COVERED
	March 1997	Final Report: June 1996 - March 1997

4. TITLE AND SUBTITLE

Spacecraft Identification by Multispectral Signature Analysis using Neural Networks

5. FUNDING NUMBERS

PE:63605F
PR: 3647
TA: AD
WU: AB

6. AUTHOR(S)

Capt Conrad J. Poelman, Stephanie R. Meltzer

7. PERFORMING ORGANIZATION NAME(S) AND ADDRESS(ES)

Phillips Laboratory
3550 Aberdeen Avenue SE
Kirtland AFB, NM 87117-5776

8. PERFORMING ORGANIZATION REPORT NUMBER

PL-TR-97-1053

9. SPONSORING/MONITORING AGENCY NAME(S) AND ADDRESS(ES)

10. SPONSORING/MONITORING AGENCY REPORT NUMBER

11. SUPPLEMENTARY NOTES

12a. DISTRIBUTION/AVAILABILITY STATEMENT

Approved for public release; distribution is unlimited.

12b. DISTRIBUTION CODE

13. ABSTRACT *(Maximum 200 Words)*

This study examines the feasibility of 1) identifying satellites by their spectral signatures and 2) developing an algorithm to automate the process. The efforts of this study focus on solving the problem of crosstagging deep space objects. Crosstagging is the misnaming of a satellite which occurs when the identity of a tracked satellite is unknown or when the identities of several satellites are commingled. This problem can occur due to variations in satellite orbits and/or delays between data collection. Sunlight reflecting off of a satellite creates a spectral signature. Satellite signatures may differ due to geometry and material properties. Spectral signatures of seven satellites were simulated using an image simulation software package and high-fidelity satellite models. These spectra took into account atmospheric degradation and were simulated for a variety of orbital parameters and different imaging times. These simulated signatures trained a neural network to identify the satellite. The trained network was able to accurately identify satellites based on their spectral signatures. This technology has application to the space analyst needing to identify satellites beyond the range of resolved imaging and detect anomalies on these objects

14. SUBJECT TERMS

Hyper-Spectral, Multi-Spectral, Neural Network, Photometry, Space Object Identification, Spectral Signature

15. NUMBER OF PAGES

32

16. PRICE CODE

17. SECURITY CLASSIFICATION OF REPORT	18. SECURITY CLASSIFICATION OF THIS PAGE	19. SECURITY CLASSIFICATION OF ABSTRACT	20. LIMITATION OF ABSTRACT
Unclassified	Unclassified	Unclassified	Unlimited

NSN 7540-01-280-5500

Standard Form 298 (Rev. 2-89)
Prescribed by ANSI Std. 239-18
28-102

THIS PAGE IS INTENTIONALY BLANK

CONTENTS

FIGURES

ABSTRACT

This study examines the feasibility of 1) identifying satellites by their spectral signatures and 2) developing an algorithm to automate the process. The efforts of this study focus on solving the problem of crosstagging deep space objects. Crosstagging is the misnaming of a satellite which occurs when the identity of a tracked satellite is unknown or when the identities of several satellites are commingled. This problem can occur due to variations in satellite orbits and/or delays between data collection. Sunlight reflecting off of a satellite creates a spectral signature. Satellite signatures may differ due to geometry and material properties. Spectral signatures of seven satellites were simulated using an image simulation software package and high-fidelity satellite models. These spectra took into account atmospheric degradation and were simulated for a variety of orbital parameters and different imaging times. These simulated signatures trained a neural network to identify the satellite. The trained network was able to accurately identify satellites based on their spectral signatures. This technology has application to the space analyst needing to identify satellites beyond the range of resolved imaging and detect anomalies on these objects.

1. INTRODUCTION

US Space Command is the organization responsible for tracking satellite orbits and monitoring their health and status. Occasionally these satellites are no longer in their expected positions due to maneuver, drift, or infrequent observations. Tracking radars and photometric observation systems can generally find and track the satellites, but may not be able to distinguish between the different satellites. In these cases it is possible for the satellites to become crosstagged, so that the operators are not certain of which satellites are which, or worse yet, incorrectly believe that they know the identities of the satellites. For low-earth orbit (LEO) satellites, ground-based optical imaging or wideband radar assets can help identify the satellites, but once satellites in deep-space orbits become crosstagged, there are few assets to help identify them. Deep space satellites are too distant to optically image, and generally lack sufficient rotation to form synthetic aperture radar (SAR) images.

This study explores the use of multi-spectral sensors to obtain additional information on deep space satellites, including health and status assessments in addition to satellite identification. Such sensors will be of maximum benefit to an operational user if they are accompanied by automated data analysis tools. For this reason, our study focuses on developing an automated spectral signature recognition algorithm, and showing that these algorithms can detect anomalous signatures. In addition to demonstrating the utility of the multi-spectral data to the operational users, these automated tools can identify patterns in the data which can determine important sensor design parameters, such as the choice of spectral bands.

We have chosen to use neural networks for spectral signature recognition and satellite identification for a number of reasons. Neural networks provide the ability to generalize from a set of examples and can be robust with respect to noisy input. Additionally, once trained to distinguish between a number of satellites, a neural network can be examined to determine which features of the input data most strongly contribute to its processing. By training the neural network with a number of input spectral bands and then examining the weights and internal connections of the network, we will be able to determine the most useful set of spectral bands for our sensor design. Since there are currently no multi-spectral space surveillance sensor data available, much of our effort to date has focused on generating simulated data for the training and testing of our algorithm.

The high-fidelity satellite models used for the simulations were created by the Phillips Laboratory. We began with models for Ekran, Gorizont and Molniya, three deep space satellites. The satellite models, two-line element sets, and ground station characteristics were then used by the Time Domain Analysis Simulation for Advanced Tracking (TASAT) code to simulate the satellite's spectral signature. These exoatmospheric signatures from TASAT were then atmospherically degraded using the Moderate Resolution Transmittance Code (MODTRAN).

A neural network was then trained to identify the different simulated spectral signatures. The ability of the neural network to generalize the results of the training was then tested by introducing previously unseen data. The results of this test showed that the network had the ability to differentiate between the satellites with minimal error.

This effort builds on a large body of previous research. Beavers collected multi-spectral and polarimetric data using three standard astronomical filters attached to an optical telescope.[1] He later performed similar experiments which investigated the effects of seasonal changes on the reflected spectra.[2] Prochko, et. al. developed non-atmospherically-degraded spectral signature simulations using the SATSIG/SATSIM simulation software, and demonstrated that the differences between the signatures of the SEASAT and DMSP satellites were substantial enough that it should be possible to distinguish between them.[3] Payne used the TASAT software to predict spectral signatures and extended the simulations to include eight different satellites, showing that it should be possible to distinguish between general classes of satellites, though perhaps not between specific models of similar design.[4] Her work also demonstrated the variation of spectral signature as a function of solar phase angle and viewing angle. Hrovat examined the use of hyperspectral imagers for observing satellites, and focused on studying the Signal to Noise Ratios (SNRs) of the expected signatures to predict that sufficient signal existed to discriminate between satellites.[5] Caudill demonstrated the use of neural networks for identifying individual materials by simulating their reflectance as it would be observed with a Sagnac interferometer.[6] In contrast, our project applies neural networks to the problem of recognizing atmospherically degraded signatures generated from high-fidelity satellite models.

In Section 2, we will describe the simulation process. Section 3 deals with our neural network procedure and Section 4 details our experiments. Conclusions and future work are discussed in Section 5.

2. SPECTRAL SIMULATION

Spectral simulations are computed using the TASAT and MODTRAN commercial off-the-shelf (COTS) software packages. Three additional modules, *write-taparams*, *write-tape5* and *convert*, automatically prepare the input files for TASAT and MODTRAN, and convert the outputs of these programs into a form acceptable for training the neural

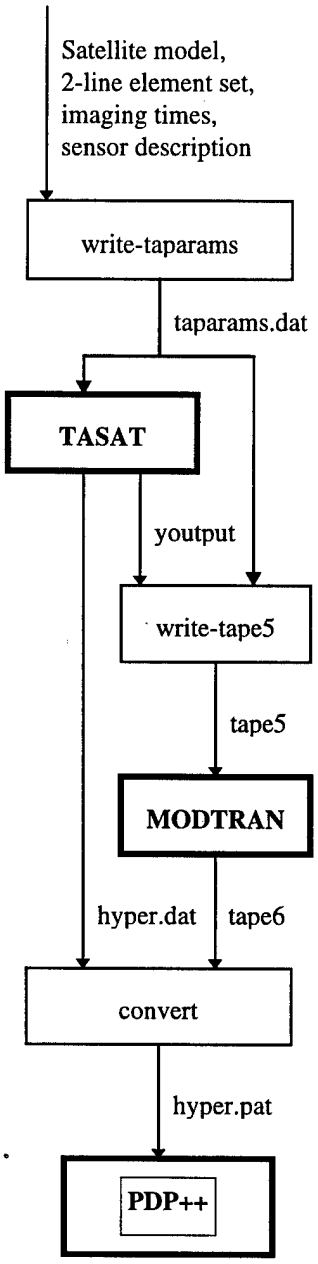

Figure 1. Simulation flow-chart

networks. The overall simulation process shown in Figure 1 is explained in the following sections.

2.1 TASAT

The Time-domain Analysis Simulation for Advanced Tracking (TASAT) software was developed by Logicon/RDA under contract to the Phillips Laboratory. TASAT was developed mainly to model electro-optical imaging and laser weapon systems effectiveness[7], but it can be used for a wide variety of simulation needs. This software provided the capability to simulate the spectral signatures we were interested in.

TASAT reads NSM satellite models, combinatorial solid-geometry (CSG) models developed by the Phillips Laboratory's Satellite Assessment Center which contain material properties and articulating part specifications in addition to basic shape information. Articulation describes the motion of certain satellite parts, such as solar panels so that they realistically move to track the sun. A separate materials database defines the wavelength dependent reflectance of each material. The quality of the simulation is limited by the quality of the information in the materials database. For some materials, reflectance values have been carefully measured and recorded in a laboratory environment over 10 nm increments, while for others, the data is only available at 100 nm intervals.

TASAT also takes as input an orbital trajectory definition in the form of a two-line element set available from US Space Command, and a series of "imaging" times. At each time step; 1) the satellite's position is propagated using the standard SGP4 propagation codes; 2) its orientation is updated based on the user-requested motion (generally nadir-pointing); 3) the position of the groundsite is computed based on the user-supplied latitude, longitude, and altitude; and 4) the sun's position is determined. A ray-tracing technique determines the spectral composition of the reflected solar light as observed at the groundsite, though the resulting signatures do not account for any atmospheric effects. Sensor parameters such as transmission of the optics and the size of the receiving aperture may also be specified to scale the resulting intensities.

The TASAT inputs are specified in the taparams.dat file. A separate defaults file referenced from the taparams.dat file contains rarely-changing program inputs and default values for TASAT parameters in the same format as the taparams.dat file. A sample taparams.dat is included in Appendix A.

TASAT generates a hyper.dat file containing the specular and diffuse components of the reflected solar light as a function of wavelength at evenly-spaced 10 nm intervals from 295 nm to 1405 nm. Additionally the output file produced by TASAT (youtput) contains many internal values which were generated in the course of its simulation, such as the position of the sun and the position of the satellite at each imaging time. These values are necessary for conversions (see Section 2.3).

2.2 MODTRAN

The MODTRAN atmospheric simulation program is used to account for atmospheric effects on the signatures. MODTRAN uses the set of fundamental molecular constants found in the HITRAN database to accurately model molecular transitions at various temperatures and pressures.[8]

The inputs to MODTRAN include time of day, ground site location, haze model (e.g. maritime, desert, rural, etc.), meteorological model (e.g. tropical, midlatitude summer/winter, 1976 US standard), moon position and phase, and so forth. Our simulations assume no rain, clouds or volcanic particles, accept the default values of wind speed and visibility for these haze models, and ignored ground-scattered light. Our input also dictated a slant path from the ground to space, single-scattering models for both the radiance and transmittance calculations, and the use of MODTRAN's internal MIE-generated database of aerosol phase functions. A sample MODTRAN input file appears in Appendix B.

MODTRAN outputs include vast amounts of chemical composition data, but the data of concern to us were the atmospheric transmittance and radiance values as a function of wave number, i.e. inverse wavelength. These output values were computed at evenly-spaced 50 cm^{-1} intervals from 7000 cm^{-1} (1429 nm) to 34000 cm^{-1} (294 nm). Transmittance is a factor from 0 to 1 specifying the fraction of light at the given wavelength which will penetrate the atmosphere. Radiance is given in units of watts per cm^2 per steridian per micron, and specifies the amount of light from the moon or the ground reradiating from the atmosphere, i.e. the basic background sky brightness at each wavelength.

2.3 PREPARATION & CONVERSION MODULES

The *write-taparams* module prepares information for TASAT. The sensor characterization information is stored in a prototype taparams.dat file for each sensor. Contained are the proper telescope aperture diameter, latitude, longitude, altitude, and site name, in addition to the general set of parameters necessary for multi-spectral simulation. The *write-taparams* module inserts the model file name, specific simulation times, and element set file name into the proper lines of the prototype file to form the final taparams.dat file used to run TASAT.

The *write-tape5* module refers to the taparams.dat file to obtain the sensor latitude, longitude, altitude, and simulation time needed to prepare the tape5 input file for MODTRAN. Since MODTRAN does not propagate satellite positions or model the encounter geometry, the zenith and azimuth angles, indicating the sensor's pointing direction, are pulled from the TASAT-generated youtput file. The position of the moon, which MODTRAN needs to compute the atmospheric reradiance values, is determined using the Vallado moon position propagation routine.[9] The lunar phase angle θ is computed from the position of the moon $\vec{R}_{moon}$, specified in earth-centered inertial coordinates (ECI), and the ECI position of the sun $\vec{R}_{sun}$, determined using the Vallado sun position propagation routine, (see Figure 2) using the dot-product formula:

$$\theta = \cos^{-1}\left(\frac{\vec{R}_{moon} \cdot (\vec{R}_{moon} - \vec{R}_{sun})}{\left\|\vec{R}_{moon}\right\| * \left\|\vec{R}_{moon} - \vec{R}_{sun}\right\|}\right)$$

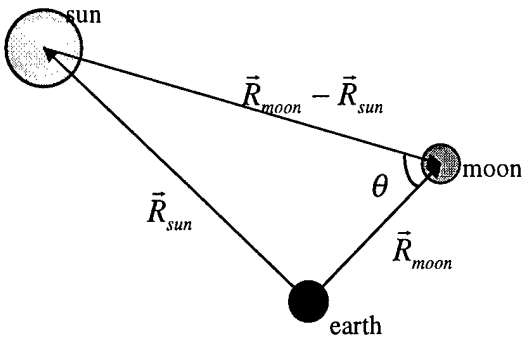

Figure 2. Lunar phase angle geometry

The *convert* module reads the MODTRAN output file, converting the radiance values from units of watts per cm^2 per steridian per micron to watts by multiplying by the sensor field of view in steradians, the area of the collector, and the spectral bandwidth of 10 nm. The exoatmospheric output signatures from TASAT are in units of watts/meter, which we convert to watts multiplying by the spectral bandwidth. The final spectral signature is computed by multiplying the exoatmospheric signatures by the transmittance and adding the radiance. Because TASAT provides data points equally spaced in wavelength and MODTRAN provides data points equally spaced in frequency, it was necessary for the *convert* module to interpolate between adjacent values in the MODTRAN output file to obtain the atmospheric transmittance and radiance values. Each atmospherically degraded signature is normalized by dividing through its maximum intensity so that the intensity values vary between 0 and 1, before writing them to the hyper.pat file for input to the neural network software.

Images of each unclassified model along with sample exoatmospheric and endoatmospheric (and normalized) signatures are shown in Figure 3, Figure 4, and Figure 5.

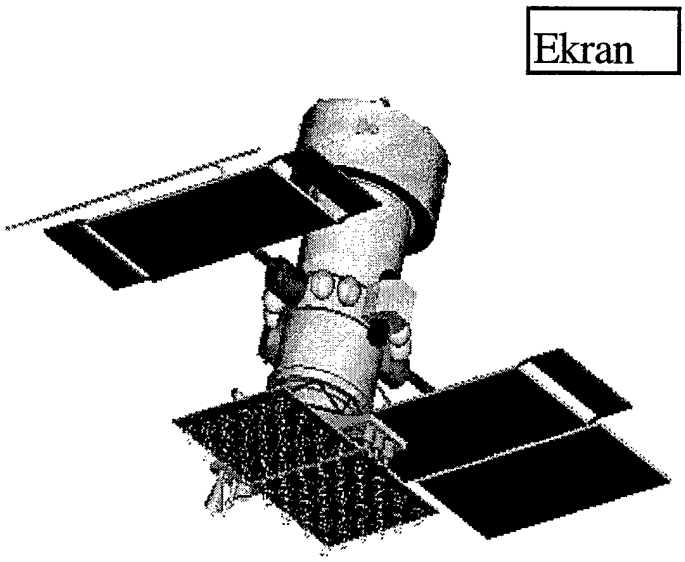

(a)

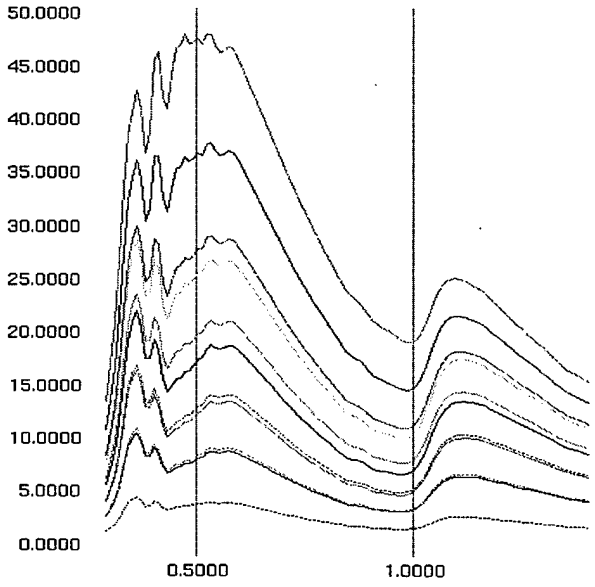

(b)

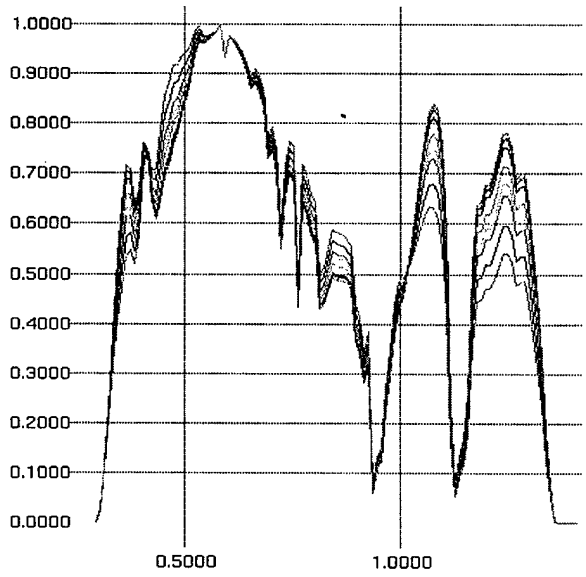

(c)

Figure 3. (a) Ekran satellite model (b) Simulated exoatmospheric signatures (in watts as a function of wavelength in microns) in a given orbit at several different imaging times (c) Signatures after accounting for the atmosphere and normalizing the intensities

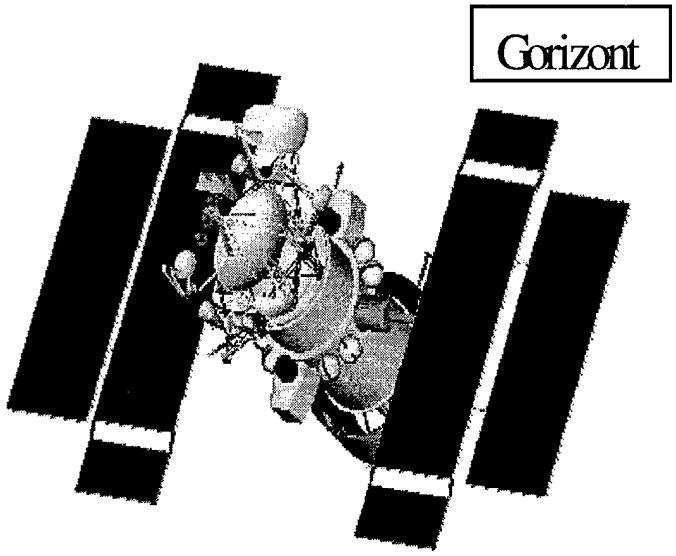

(a)

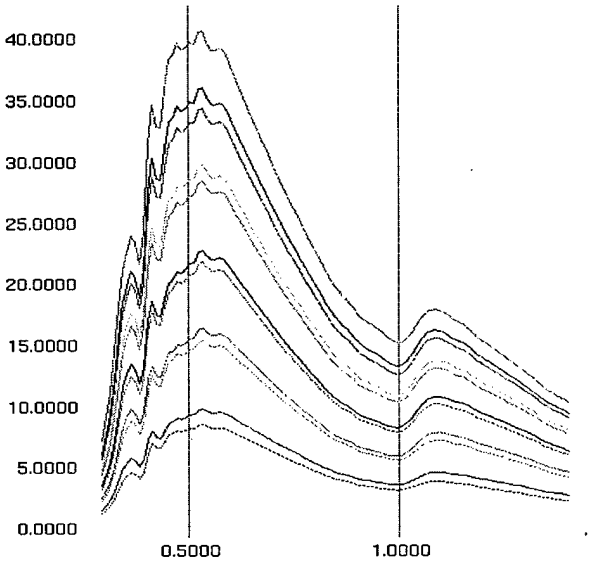

(b)

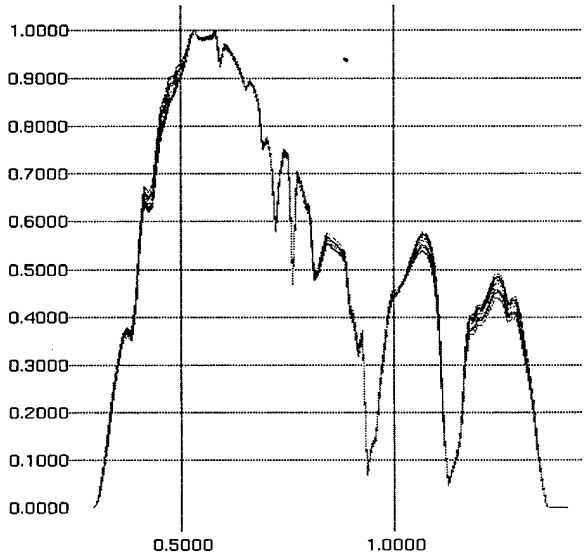

(c)

Figure 4. (a) Gorizont satellite model (b) Simulated exoatmospheric signatures (in watts as a function of wavelength in microns) in a given orbit at several different imaging times (c) Signatures after accounting for the atmosphere and normalizing the intensities

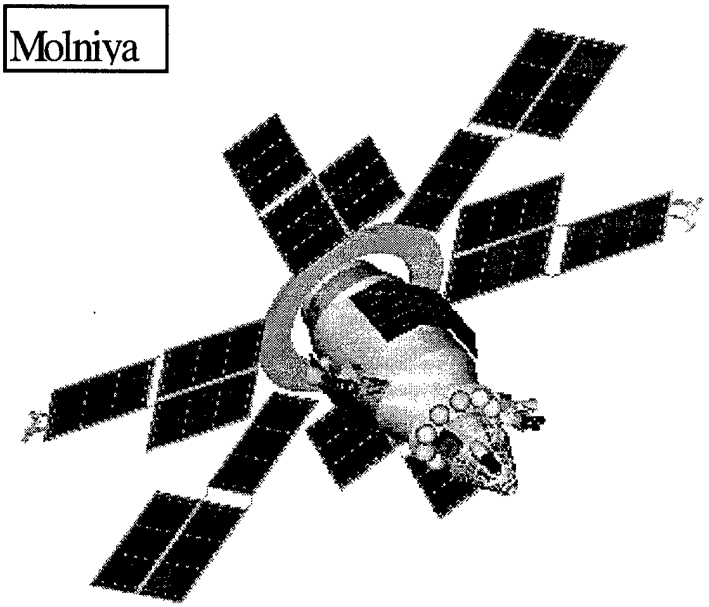

(a)

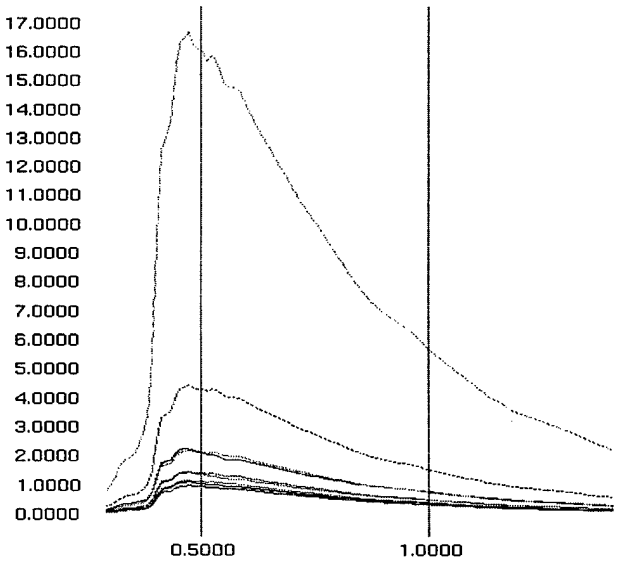

(b)

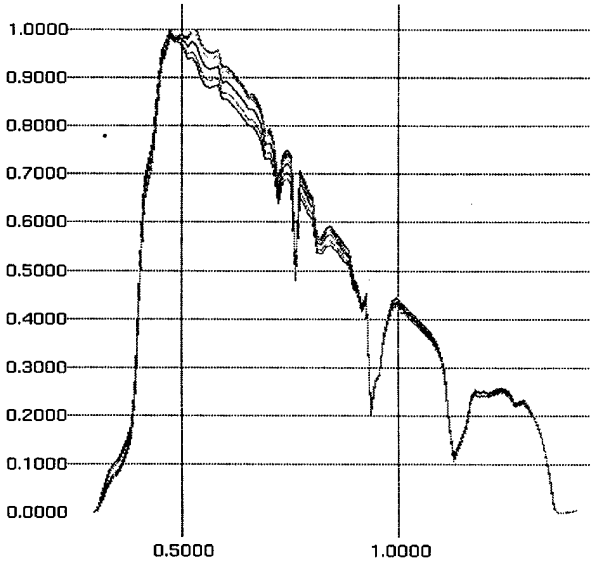

(c)

Figure 5. (a) Molniya satellite model (b) Simulated exoatmospheric signatures (in watts as a function of wavelength in microns) in a given orbit at several different imaging times (c) Signatures after accounting for the atmosphere and normalizing the intensities

3. NEURAL NETWORK RECOGNITION TECHNIQUE

3.1 NEURAL NETWORKS

Neural networks are computational devices whose basic design was inspired by neurological evidence of the computation performed by neurons in humans and other primates. They are useful computational tools which learn mappings from inputs to outputs based on training examples. Each layer of a standard feed-forward network consists of a number of nodes which are connected to each node in the subsequent layer. Each node computes a single output value by applying a simple function to its inputs, and each connection between nodes has a variable weight associated with it. During the training process, input patterns and their corresponding target output patterns are presented to the network, and the network's weights are updated via the backpropagation algorithm. The adjustment of the weights is based on the calculations of the derivative of the error in the output of the network with respect to each weight.[10]

3.2 PDP++

The Parallel Distributed Processing (PDP++) neural network freeware package, developed at Carnegie Mellon University, uses a backpropagation-type network like the one described above. PDP++ consists of both a C++ class library and an extensive graphical user interface which allows the user to modify the network architecture, train the network, examine specific weights, and so forth.

3.3 SPECTRAL SIGNATURE RECOGNITION ARCHITECTURE

The neural network architecture which we employed for spectral signature recognition consists of three layers. The input layer consists of 112 input nodes corresponding to the 112 wavelength bands (10 nm each from 295 nm to 1405 nm) generated by simulation. The single hidden layer consists of as few nodes as possible while still allowing for generalization. The output layer contains of a node corresponding to each satellite that the network is being trained to identify, either three or seven in our experiments. An example of the network structure can be seen in Figure 6.

The correct output pattern is defined by assigning the value of one to the output node corresponding to the satellite, and assigning values of zero to the other nodes. When a signature is presented to the network, the output of the network may not exactly match this pattern, so we classify the signature according to the most strongly activated output node. The degree to which the actual output pattern differs from a correct output pattern can be used as a qualitative measure of the network's confidence in its classification. The distribution of this difference for each node of the output layer can provide further information regarding the network's confidence; for example, if two nodes are highly activated and the remaining nodes are near zero, then the network is indicating that the signature may come from either of the satellites corresponding to the two highly activated nodes, but is unlikely to be from any of the other satellites.

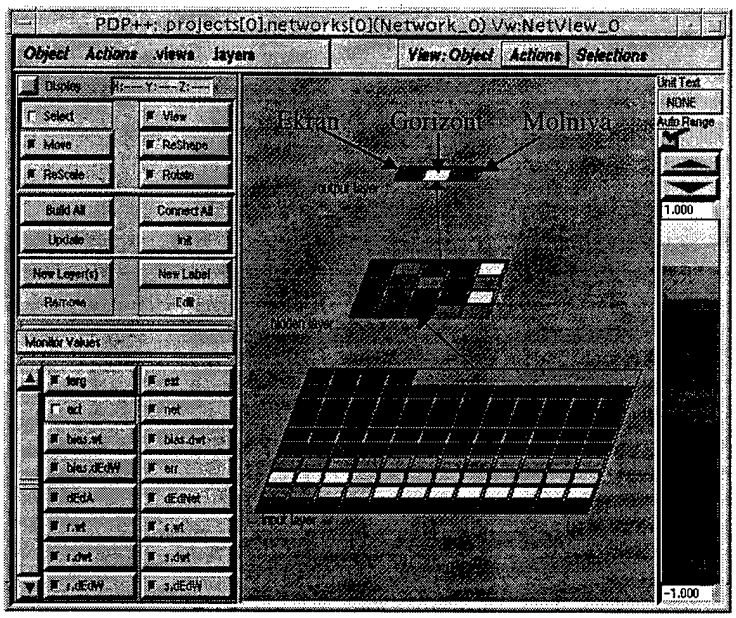

Figure 6. PDP++ Neural network screen

3.4 TRAINING

Training takes place by repeatedly exposing the network to a series of events. During each event, a training signature for a given satellite is presented to the network, and the initially random weights of the connections between the nodes are adjusted in an effort to produce the correct output pattern for the satellite. The sum-of-squares error between the network's output and the correct output is measured at each time step, and training continues until the error reaches a stable and hopefully low plateau.

Various parameters can be modified to effect the training process. The learning rate (lrate) controls how fast the weights are updated along the computed error gradient. It is usually less than one, but harder problems require smaller values. The momentum parameter (mom) determines how much of the previous weight change will be retained in the present weight change computation. The momentum parameter allows learning to "pick up speed" if the weight changes all head in the same direction. This can allow the network to learn faster if the problem is a rather easy one, but may be detrimental if the problem is tough because the network may rush past an important bump in the learning curve. Typical values for momentum are .5 to .9.[11]

A low sum-of-squares error after completing the training process indicates that the network has successfully learned to produce the correct output patterns when given an input signature from the training set. A high training error can indicate a number of things. It may indicate that the number of hidden nodes is too small, so the network lacks sufficient "memory" to learn. It may also indicate that there is not enough information in the training set to learn the differences between the satellites, possibly because certain satellites have nearly identical signatures.

3.5 GENERALIZATION TESTING

It is important to test the network's ability to generalize by measuring its performance when previously unseen signatures are introduced. If most of the unseen signatures are classified correctly, then the network has generalized from the training set. If the network performs badly when presented with the new signatures, it may indicate that the network has too many hidden nodes and has simply memorized the training set without performing any generalization. It may also indicate that the training set was too narrow, meaning that certain signatures presented during generalization testing bore little resemblance to the original signatures used for training.

4. EXPERIMENTS

Four experiments were performed, varying the number of satellites the network was trained to identify and the inclusion or exclusion of atmospheric effects, as shown in Table 2. We chose to model the three Ground-based Electro-Optical Deep Space Surveillance (GEODSS) sites because of their interest to Space Command, using the site parameters listed in Table 1.

	Aperture (m)	MODTRAN Haze Model	MODTRAN Meteorological Data
Socorro	1.0	desert	midlatitude
Maui	1.0	maritime	tropic
Diego Garcia	1.0	maritime	tropic

Table 1. Sensor-specific parameters

In order to train the neural network, it was necessary to generate large amounts of simulated data. Typical two-line element sets for the satellites under consideration were acquired from Space Command. These orbital trajectories were analyzed using the Satellite Orbit Analysis Program (SOAP) to determine from which ground site and at which imaging times the satellite could be viewed under proper illumination conditions. Each orbit was used to define a number of *scenarios*, (a particular orbit, ground station, and simulation time), spacing simulation times at approximately one hour intervals between the orbit's first and last valid imaging times. Signatures were then simulated by placing each satellite model in each scenario.

Half of the simulated data was used to train the neural network, while the remaining data was reserved for generalization testing. PDP++ repeatedly presented each training example to the network, updating the networks weights using the backpropagation algorithm, and displaying the resulting sum-of-squares error between the network outputs and the correct outputs. When this error reached a low and stable level, the training process was stopped. (see Figure 7)

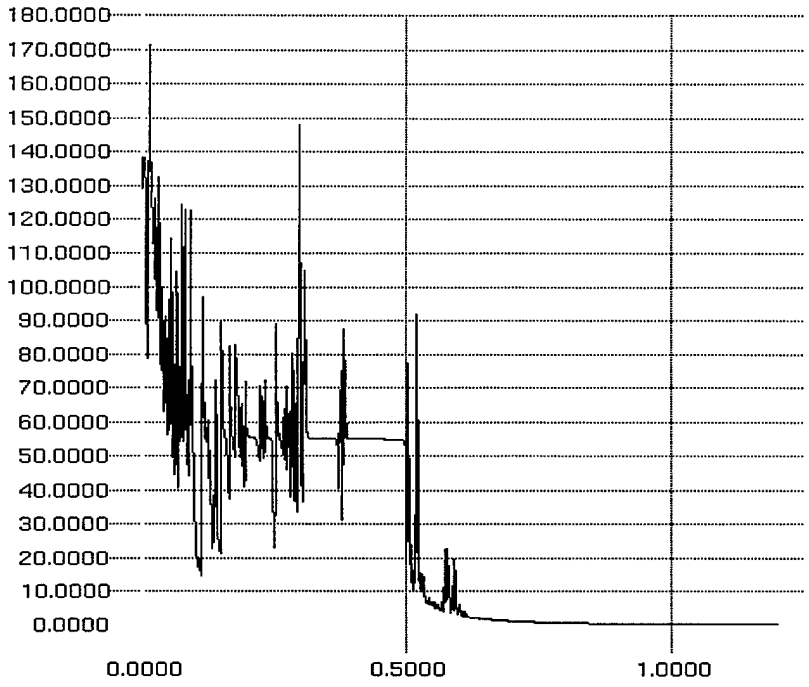

Figure 7. Network training error versus time

Satellites	atm	hidden nodes	lrate	mom	training examples	epochs	error	testing examples	success rate
3	no	15	0.05	0.4	133	2000	0.0452	132	100%
3	yes	15	0.05	0.4	133	2000	0.0415	132	100%
7	no	20	0.01	0.4	329	10000	25.418	329	94%
7	yes	20	0.01	0.4	329	10000	21.313	377	92%

Table 2. Neural network parameters

During the training of the network, we examined some of the cases in which the network had difficulty learning to identify a particular case. In some instances, we found these signatures to be similar to the spectral signature of the sun, shown in Figure 8. In these cases, it is possible that the viewing angle was such that the signature was dominated by the solar panels and therefore the signature was not indicative of the entire satellite.

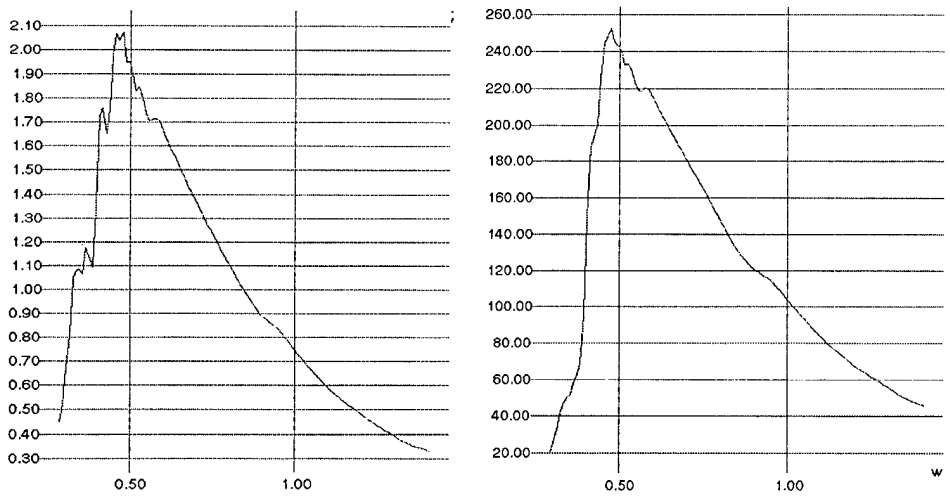

(a) (b)

Figure 8. (a) Solar Spectrum (b) Mis-classified Gorizont spectral signature

5. CONCLUSIONS

5.1 SUMMARY

This research project has demonstrated the application of neural network techniques for the automatic identification of deep space satellites based on their multi-spectral signatures. We have developed tools for the automatic generation of large sets of simulated spectral signatures from high-fidelity satellite models and including atmospheric effects. We have demonstrated that neural networks have the ability to generalize from training examples and identify previously unseen signatures with high probability.

5.2 FUTURE WORK

Whenever a satellite's signature is observed, the viewing angle and solar illumination angles will be known but we do not provide this information to the network. Similarly, we currently normalize the intensities of the signatures but do not provide the unnormalized magnitudes of the signatures to the network. Recognition performance may be improved by adding these values as inputs to the neural network.

The simulation will be upgraded to include additional signature degradation phenomena, such as photon shot noise and any noise associated with the sensor or sensor readout. Alternate normalization techniques which are more robust with respect to noisy data will also be considered.

We are currently investigating various filter and sensor technologies in preparation for the experimental stage of our project, in which we plan to use a set of off-the-shelf filters mounted into the filter wheel of a GEODSS telescope. We

are examining the weights of the network to help determine the correct filter bands to use for a multispectral experiment. We will update our simulations and neural network architecture to validate the candidate filter set.

APPENDIX A

TASAT input file: taparams.dat

```
*************** THIS SECTION IS REQUIRED TO RUN TASAT ********************
>> VERSION 6.65 << TASAT TIME AVERAGE SIMULATION CONFIGURATION FILE
TA_HYPER.DFT          TIME AVERAGE CONFIGURATION DEBUG/DEFAULT PARAMETERS
../taparams/                              PATH TO DEBUG/DEFAULTS FILE
*****************************************************************************

CREATED BY:  Phillips Lab
DATE:        15 Jan 1196
NOTES:       HYPER SPECTRAL SIGNATURE GENERATION EXAMPLE:
SENSOR BAND IS EVERY 10 nm:  FROM 295 nm, TO 1405 nm
HYPER-SPECTRAL CURVE IS IN FILE NAMED:  hyper.dat
OBJECT IS EKRAN
OBSERVER IS DIEGO GARCIA

******************** TOP LEVEL SIMULATION PARAMETERS ****************
SIMULATION CONTROLS:
11-MAR-96      simdate        TODAY'S DATE (FREE FORMAT STRING)
USEFUL         msgenable      MESSAGE ENABLE (NONE;IMPORtant;USEful;DIAGnostic)
SCREEN         msgdevices     MESSAGE DEVICES (NONE;SCREEN;DISK;BOTH)
screen.msg     msgfilename    MESSAGE DISK FILENAME (LOCAL DIRECTORY ONLY)
END BLOCK:

SIMULATION TIMING:
1996           epochyear      YEAR OF SIMULATION EPOCH (GMT @ SIMULATION T=0)
7              epochmonth     MONTH OF SIMULATION EPOCH (1:12;GMT)
7              epochday       DAY OF SIMULATION EPOCH (1:31;GMT)
1515.30        epochtime      GREENWICH MEAN SOLAR TIME AT SIM EPOCH (HHMM.SEC)
0.000          epochoffset    SIMULATION EPOCH OFFSET (SEC;positive ADVANCES TIME
*TIMING_EQUAL_INCREMENTS:
3600            clockdelta     tasattu-CLOCK Y(*) OUTPUT INCREMENT TIME (SEC)
24600           clockend       tasattu-CLOCK SIMULATION FINISH TIME (SEC)
NULL            presimfile     tasattu-PRESIM FILE (NULL=none)
END BLOCK:

GLOBAL VARIABLES:
256            npixels        NUMBER OF PIXELS FOR ALL PSFs AND IMAGEs (NOT FPAs)
```

```
INCREMENT      imagefilenum  IMAGE OUTPUT FILE NAMING (OVERWRite;INCREMent)
UNCLASS        classlevel    SIMULATION OUTPUT LEVEL OF CLASSIFICATION
END BLOCK:

************************** TARGET *********************************
TARGET:
*MODEL:
ekran.nsm      targfil       TARGET MODEL (*.NSM) FILENAME
../multi-spec-data/models/   targpath      PATH TO TARGET MODELS
00000          targsscid     TARGET MODEL SSC ID NUMBER
NOMINAL        brdfprop      BRDF PROPERTIES (NOMINAL;LAMBERTian all materials)
0              targwidth     MAXIMUM APPROXIMATE TARGET FULL ANGULAR WIDTH (RAD)
0.0            targrot1      1st FIXED ROTATION ANGLE ABOUT BODY AXIS-I (DEG)
0.0            targrot2      2nd FIXED ROTATION ANGLE ABOUT BODY AXIS-J (DEG)
0.0            targrot3      3rd FIXED ROTATION ANGLE ABOUT BODY AXIS-K (DEG)
123            targrotseq    I,J,K AXIS SEQUENCE (1=I;2=J;3=K) (ABOUT NEW AXES)
0.0            targoffsetx   MODEL OFFSET ALONG BODY X AXIS (M) (EG. TO SHIFT CM)
0.0            targoffsety   MODEL OFFSET ALONG BODY Y AXIS (M)
0.0            targoffsetz   MODEL OFFSET ALONG BODY Z AXIS (M)
*TRAJECTORY:
ORBIT       trajectory    TRAJECTORY TYPE (ORBIT;GNDSITE;SNAPSHOT;6DOF-THIST;)
NORAD       latitude      GROUNDSITE GEODETIC LATITUDE (DEG) [+=NORTH]
gor01.dat   elsetfile     NORAD element set file
../multi-spec-data/elsets/    elsetpath     NORAD element set file path
*ATTITUDE:
NADIR       attitude      ATTITUDE TYPE (GNDSITE_NWZ;GNDSITE_SEZ;EARTH_IJK;...)
END BLOCK:

************************** GROUND SITE #1 *************************
ELECTRO-OPTICAL SYSTEM 1:
DG             sitename      EO #1 SITE/SYSTEM NAME
*RECEIVER OPTICS:
1.0            aperturediam  RECEIVER TELESCOPE CLEAR APERTURE DIAMETER (M)
0.15           obscurediam   RECEIVER TELESCOPE OBSCURATION DIAMETER (M)
1.0            beammag       BEAM EXPANDER MAGNIFICATION (AFOCAL RATIO)
*GIMBAL:
ELEL       gimbaltyp     GIMBAL TYPE (NONE;AZEL=el/az;ELEL=el/el;APD=az/pol/dec)
0.0        outgimbmntang STATIC OUTER GIMBAL MOUNT ANGLE (AZIMUTH; DEG FROM X-
AXIS)
0.0        apdtipangle   STATIC POLAR AXIS TIP-DOWN ANGLE (DEG FROM Z-AXIS,APD
only)
```

```
NO          coudeflg  INCLUDE COUDE' OPTICAL PATH TO SENSORS? (YES;NO=ON GIMBAL)
NO      inclderotoptics INCLUDE DEROTATION OPTICS? (NO;YES=X-AXIS ALONG VEL;APD)
*TRAJECTORY:
GNDSITE    trajectory    TRAJECTORY TYPE (ORBIT;GNDSITE;SNAPSHOT;6DOF-THIST;...)
-7.41      latitude      GROUNDSITE GEODETIC LATITUDE (DEG) [+=NORTH]
72.45      longitude     GROUNDSITE LONGITUDE (DEG) [-=WEST OF GREENWICH]
23         altitude      GROUNDSITE ALTITUDE ABOVE MEAN SEA LEVEL (M)
YES        earthrotflg   INCLUDE EARTH ROTATION IN CALCULATIONS (YES;NO)
*ATTITUDE:
GNDSITE_NWZ  attitude     ATTITUDE TYPE (GNDSITE_NWZ;GNDSITE_SEZ;EARTH_IJK;...)
END BLOCK:


CAMERA 1:
ON         camenable     CAMERA #1 ENABLE (ON;OFF) (OFF inhibits everything)
GEODSS     sensorsysname SENSOR SYSTEM NAME
cam1spec.dat camspectfil     SPECTRAL CHARACTERISTICS FILENAME ('NULL' IF NOT
NEEDED)
../data/   camspectpath  PATH TO SPECTRAL FILE
NO         rescaletomag  RESCALE PRISTINE IMAGE TO STELLAR MAGNITUDE (YES;NO)
0.0        stellarmag    EQUIVALENT STELLAR MAGNITUDE (UNITLESS, if yes)
0.043      camrenderres  PRISTINE RENDERING RESOLUTION (RAD or METERS) (0.0=CODE
SETS)
*POLARIZATION FILTER:
NONE       campoltyp     POLARIZER (NONE;X-LINEAR;RIGHT;EXEY;STOKES;...)
0.0        campoladmitang              ADMITTANCE AXIS ANGLE WRT X-AXIS OF FPA
*SPECTRAL FILTER TRANSMISSION:
FLAT       specshape     SPECTRAL FILTER SHAPE TYPE (FLAT;GAUSSIAN;DISK)
0.850E-6   specpasswave  PASSBAND NOMINAL CENTER WAVELENGTH (M)
1.110e-6   specpasswidth PASSBAND SPECTRAL WIDTH (M) (EDGES;HALF_POWER POINTS)
1.0        spectrans     SPECTRAL FILTER TRANSMISSION (0:1)
0.850E-6   spectranswave WAVELENGTH FOR SPECTRAL TRANSMISSION VALUE (M)
*OPTICS TRANSMISSION:
CONST      optshape      OPTICAL TRANSMISSION SHAPE TYPE (CONSTant;DISK)
1.0        opttrans      OPTICAL TRANSMISSION (0:1)
0.850E-6   opttranswave  WAVELENGTH FOR OPTICAL TRANSMISSION (M)
*FPA READOUT ELECTRONICS:
0.000       readoutdelta  SINGLE PIXEL READOUT TIME DELTA (SEC) (TO DIGITIZE 1
PIXEL)
0.001      readoutupdate SHORT TERM EXPOSURE UPDATE TIME (SEC) (TO CAPTURE
DYNAMICS)
0.001      readoutdwell  TOTAL OPTICAL EXPOSURE DWELL TIME (SEC)
0.001      readoutframe  FPA READOUT FRAME TIME (SEC) (1/OUTPUT FRAME RATE)
```

```
1.0         readoutgain    IMAGE-INTENSIFIER GAIN (1.0=IF NO INTENSIFIER)
CONST       readoutqtype   QUANTUM EFFICIENCY CURVE TYPE (CONSTant;DISK)
1.0         readoutqe      QUANTUM EFFICIENCY (Qe) [e/photon]
0.850E-6    readoutqewave  WAVELENGTH OF QUANTUM EFFICIENCY (M)
0.0         readoutrmsqe   % RMS Qe RESIDUAL SPATIAL NONUNIFORMITY (1-sigma)
0.0         readoutdarki   MEAN DARK CURRENT (e/sec) PER PIXEL
0.0         readoutdarkrms    % RMS DARK CURR RESIDUAL SPATIAL NONUNIFORMITY (1-
sigma)
0.0       readoutpost    MEAN DARK CURRENT DIGITAL POST REMOVAL (e/sec) PER PIXEL
1.0E10      readoutsat     PHOTOSITE (QUANTUM WELL) HARD SATURATION LIMIT (e)
0.0         readoutsatshapex   SAT SPILL GAUSSIAN SHAPE, 1-SIGMA ALONG X-AXIS
0.0         readoutsatshapey   SAT SPILL GAUSSIAN SHAPE, 1-SIGMA ALONG Y-AXIS
0.0         readoutsatloss    % SATURATION CHARGE LOSS (CHARGE SPILLED TO ADJACENT
PIXELS)
1.0         readoutcte     CHARGE TRANSFER EFFICIENCY PER SHIFT (EG. 0.999)
NONE        readoutnoisemdl  ELECT NOISE MODEL (NONE;SHOT;ELECT;BOTH;SNR peak
0.0         readoutrss        RSS OF ALL DETECTOR/AMP/READOUT NOISES, 1-SIGMA (e)
0.0         readoutpeaksnr    PEAK PIXEL SNR (if PEAK snr)
photo       readoutadcmode    ADC OUTPUT MODE (PHOTO-electrons;digital COUNTS)
12          readoutadcbits    ANALOG TO DIGITAL CONVERTER OUTPUT BITS
4095.0      readoutelectrons ADC FULL SCALE # ELECTRONS PER PIXEL (e)
*VIDEO OUTPUT:
WORD      videotype    VIDEO IMAGE TYPE (BYTE(0-255);WORD(0-32K);REAL;ASCII;TIFF)
NONE        imageflip      IMAGE FLIP CONTROL (NONE;ROWs;COLumns;BOTH)
no          outputmoments OUTPUT IMAGE MOMENTS (NO;YES)
0.0         uirad          UNIT IRRADIANCE......(UIRAD000.IMG) (SEC)
0.0         actsl          PAS SOLAR ILLM.......(ACTSL000.IMG) (SEC)
1.0         actpr          PRISTINE U+P.........(ACTPR000.IMG) (SEC)
0.0         psfad          IMAGING PSF..........(PSFAD000.IMG) (SEC)
0.0         actcv          DEGRADED.............(ACTCV000.IMG) (SEC)
0.0         actfp          DETECTOR.............(ACTFP000.IMG) (SEC)
0.0         depth          DEPTH IMAGE..........(DEPTH000.IMG) (SEC)
0.0         actax          AUXILIARY IMAGE......(ACTAX000.IMG) (SEC)
0.0         actmp          MAP-2 TRACK IMAGE....(ACTMP000.IMG) (SEC)
0.0         actsv          SIEVE GATE IMAGE.....(ACTSV000.IMG) (SEC)
END BLOCK:

DOWNLINK ATMOSPHERICS - CAMERA 1:
*ATMOSPHERIC TRANSMISSION BETWEEN CAMERA AND TARGET:
CONST       camtargtransspect   SPECTRAL SHAPE TYPE (CONSTant;DISK)
1.0         camtargtrans  ATMOSPHERIC TRANSMISSION TARGET TO CAMERA 1 (0-1)
```

```
0.850E-6  camtargwave   WAVELENGTH FOR ATMOSPHERIC TRANSMISSION (M)
END BLOCK:

************************** SOLAR LIGHT SOURCE **************************
LAMP 3:
ON        lampenable    LAMP ENABLE (ON;OFF)
yes       earthobscuration INCLUDE EARTH OBSCURATION? (YES;NO)
lmp3spec.dat   lampspectfil   SPECTRAL CHARACTERISTICS FILENAME ('NULL' IF NOT
NEED
../data/   lampspectpath PATH TO SPECTRAL DATABASE
*EMISSION CHARACTERISTICS:
DISK     lampemisstyp  LAMP EMISSION TYPE (LASER;BLKBDY;DISK)
0.0   lampintpower TOTALINTEGRATED OPTICAL PWR EMITTED (WATTS, ALL WAVELENGTHS)
*LAMP OPTICAL TRANSMISSION:
FLAT      opttransshape      SPECTRAL FILTER SHAPE TYPE (FLAT;GAUSSIAN;DISK)
2.0E-9    opttranspasswave   CUTON SHORT WAVELENGTH (M)
1.6E-5    opttranspasswid    CUTOFF LONG WAVELENGTH (M)
1.0       opttrans       LAMP OPTICS TRANSMISSION (0:1)
1.000E-6  opttranswave  CENTER WAVELENGTH FOR OPTICS TRANSMISSION (M)
*TRAJECTORY:
SUN       trajectory    TRAJECTORY TYPE (ORBIT;GNDSITE;SUN;MOON;SNAPSHOT;6DOF-
THIST)
*ATTITUDE:
OBJ_POINT  attitude     POINTS SOLAR Z-AXIS AT TARGET CENTER
END BLOCK:

UPLINK ATMOSPHERICS - LAMP 3:
*ATMOSPHERIC TRANSMISSION BETWEEN LAMP AND TARGET:
CONST     camtargtransspect   SPECTRAL SHAPE TYPE (CONSTant;DISK)
1.0       camtargtrans  ATMOSPHERIC TRANSMISSION (0.0:1.0)
1.000E-6  camtargwave   WAVELENGTH FOR ATMOSPHERIC TRANSMISSION (M)
END BLOCK:

********************** RENDERING BLOCK CONTROLS **********************

RENDER BLOCK CONTROLS:
NORMAL    rendermode   RENDER OPERATING MODE (NONE;NORMal;STATS;DIAG-RAY;DIAG-
PIXEL)
WATTS     renderunits      RENDERED IMAGE UNITS (WATTS;RADiance)
0.1       rendertimedelt   RERENDERING TIME STEP (dT >= 0.1 sec)
FAST      renderfidelity   RENDERING FIDELITY/SPEED MODE (FAST=LOW FI) [NOR
COSINE    auximagetyp      AUX IMAGE TYPE (NONE;TEMP;BRDF;COSINE;...)
```

```
1          auximagelamp      LAMP # FOR BRDF AUX IMAGE
1          bufferplanenum    LIGHT BUFFER PLANE # TO OUTPUT IN AUX IMAGE
NO         retroenable    INCLUDE TARGET RETRO-REFLECTORS IN SIGNATURE? (YES;NO)
NO         thermtraceenable  DO THERMAL RAY TRACING (YES;NO)
END BLOCK
END OF PARAMETERS:
```

APPENDIX B

MODTRAN input file: tape5

```
T   1    3    2   0    0    0    0    0    0    0    0    0    1   0.000   0.00
f   0f   0       .000
    4     2     0     0     0     0       0.000     -1.000       0.000       0.000
0.023
     0.023     0.000    15.125     0.000     0.000     0.000     0
    0    2  214    1
    -7.410      72.450      -9.748    156.540      14.682      -5.731      16.891
0.000
      7000     34000        50        50
    3
     0.023     0.000    15.156     0.000     0.000     0.000     0
    0    2  214    1
    -7.410      72.450      -9.575    142.113      15.682     -17.815      17.460
0.000
    3
     0.023     0.000    15.567     0.000     0.000     0.000     0
    0    2  214    1
    -7.410      72.450      -9.400    127.685      16.683     -26.186      18.029
0.000
    3
     0.023     0.000    15.861     0.000     0.000     0.000     0
    0    2  214    1
    -7.410      72.450      -9.224    113.257      17.683     -30.509      18.599
0.000
    3
     0.023     0.000    15.705     0.000     0.000     0.000     0
    0    2  214    1
    -7.410      72.450      -9.048     98.827      18.683     -31.051      19.170
0.000
    3
     0.023     0.000    14.987     0.000     0.000     0.000     0
    0    2  214    1
    -7.410      72.450      -8.870     84.397      19.683     -27.897      19.741
0.000
    3
     0.023     0.000    13.833     0.000     0.000     0.000     0
    0    2  214    1
    -7.410      72.450      -8.692     69.965      20.683     -20.592      20.313
0.000
```

```
    3
     0.023     0.000    12.649     0.000     0.000     0.000     0
    0    2  214    1
    -7.410     72.450     -8.513     55.533     21.683     -8.244     20.886
0.000
    3
     0.023     0.000    12.120     0.000     0.000     0.000     0
    0    2  214    1
    -7.410     72.450     -8.333     41.099     22.683      9.174     21.458
0.000
    3
     0.023     0.000    12.908     0.000     0.000     0.000     0
    0    2  214    1
    -7.410     72.450     -8.152     26.665     23.683     28.318     22.031
0.000
    3
     0.023     0.000     0.000     0.000     0.000     0.000     0
    0    2  215    1
    -7.410     72.450    -12.165      8.252      0.000      0.000      8.827
0.000
    0
```

REFERENCES

[1] W.I. Beavers, Optical Monitoring of Geosynchronous Satellites, MIT Lincoln Laboratories Project Report STK-233, 27 January 1995.

[2] W.I. Beavers, UBV Photometry of Geosynchronous Satellites, MIT Lincoln Laboratories Project Report STK-241, 19 October 1995.

[3] A.E. Prochko, M. Culpepper, S. Durham, J. O'Hair, Spectral Signatures Predicted from Detailed Satellite Models, Proceedings of the 1995 Space Surveillance Workshop, MIT Lincoln Laboratories Project Report STK-235 vol. 1.,28-30 March 1995.

[4] T. Payne, et al, Spectral Signatures for Deep Space SOI: A Status Report, Deep Space Spectral Sensing Working Group, 1 December 1995.

[5] D. Hrovat, Hyperspectral Analysis of Space Objects: Signal to Noise Evaluation, Air Force Institute of Technology Thesis AFIT/GSO/ENP/93D-02, December 1993.

[6] E.L. Caudill, Satellite Surface Material Composition from Synthetic Spectra, Air Force Institute of Technology Thesis AFIT/GEO/ENG/94-D02, December 1994.

[7] Crockett, G., et al, The Time-Domain Analysis Simulation for Advanced Tracking (TASAT) Users Manual Version 6.6, Logicon R&D Associates, July 1995.

[8] Anderson, G., et al, FASCONDE/MODTRAN/LOWTRAN: Past/Present/Future, "18th Annual Review Conference on Atmospheric Transmission Models", 6-8 June 1995.

[9] D.Vallado, Methods of Astrodynamics: A Computer Approach - Version 4.0, 14 March 1992.

[10] K.L. Priddy, Introduction to Neural Networks, Accurate Automation Corporation.

[11] Dawson, C., R. O'Reilly, J. McClelland, The PDP++ Software Users Manual Version 1.1, Carnegie Mellon University, 28 May 1996.

DISTRIBUTION LIST

AUL/LSE Bldg 1405 - 600 Chennault Circle Maxwell AFB, AL 36112-6424	1 cy
DTIC/OCP 8725 John J. Kingman Rd, Suite 0944 Ft Belvoir, VA 22060-6218	2 cys
AFSAA/SAI 1580 Air Force Pentagon Washington, DC 20330-1580	1 cy
PL/SUL Kirtland AFB, NM 87117-5776	2 cys
PL/HO Kirtland AFB, NM 87117-5776	1 cy
Official Record Copy PL/WSAT/Capt. Conrad J. Poelman	10 cys
PRC Inc. P.O. Box 1159 Socorro, NM 87801	3 cys
MIT Lincoln Laboratory P.O. Box 1707 Socorro, NM 87801	2 cys
W. J. Schafer Associates, Inc. 2000 Randolph Road, SE Suite 205 Albuquerque, NM 87106	1 cy